**SALT DISTRIBUTION FROM FREEZING INTRUSIONS IN ICE SHELLS ON OCEAN WORLDS.**

M. Naseem [1], M. Neveu [1,2], S. Howell [3], E. Lesage [3], M. M. Daswani [3], and S. D. Vance [3]. [1]University of Maryland, College Park (mnaseem@umd.edu), [2]NASA Goddard Space Flight Center (marc.f.neveu@nasa.gov), [3]Jet Propulsion Laboratory, California Institute of Technology.

**Introduction:** Several icy moons and dwarf planets of the solar system appear to host past or present bodies of subsurface salty liquid water. Observations of surface composition and landforms suggest mechanisms of convective or cryovolcanic transport. There are multiple science motivations for understanding these transport processes through ice shells, including gaining insight into how material is delivered to the surface, and informing the connection between surface expression and subsurface conditions to unveil potential indicators of habitability. Transport processes are affected by the thermo-mechanical properties of ice shell materials and hence, by the chemistry and compositional structure of ice shells, which remain poorly constrained. As liquid water intruding upwards into the icy outer shells of these worlds undergoes partial or full freezing, it forms ice and non-ice solids. To understand the influence of these compositional heterogeneities on transport through ice shells, we numerically model the spatial distribution of the formed water-ice, salts, methane hydrates, amorphous silica, and the residual briny solutions, as a function of the degree of freezing.

**Methods:** The spatial distribution of ice, salts, and liquid within a freezing fluid intrusion into an ice shell is determined in two major steps. First, we compute the chemical sequence of forming species as a function of decreasing temperature. Second, we distribute the formed solids according to their density, the shape of the intrusion, and assumptions about the relative rates of crystallization, settling and mixing.

For the chemical calculations, we use the PHREEQC v3 code [1] with thermodynamic data either derived by [2,3] or converted by [4] from prior work [5-7]. These chemical calculations are independent of time, and it is simply assumed that temperatures decrease with time. Spatial distributions are obtained by converting molar amounts of formed chemical species to volumes of ice, salts, and solution.

We considered freezing in a cryomagma chamber (assumed spherical for simplicity) within an ice shell. If freezing is faster than salt formation, e.g., if the fluid intrusion encounters a much colder surrounding ice shell, the forming salts are incorporated in the thickening chamber wall (Fig. 1a). Otherwise, the solid distribution can span the endmembers of Fig. 1b (no settling) and 1c (no mixing).

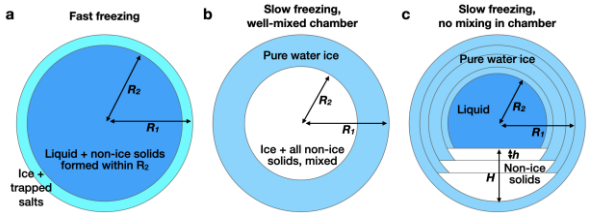


***Figure 1. Possible end-member distributions of materials in freezing spherical chamber showing chamber radii ($R_1$, $R_2$) and sediment height (H).*** *(a) Fast freezing by fractional crystallization. (b) Slow freezing by equilibrium crystallization with salts excluded from ice and well mixed with chamber fluid. (c) Slow freezing with salts settling by density, resulting in fractional crystallization.*

**Results:** Solid compositions were simulated from the freezing of end-member compositions for Europa's ocean obtained by [8]. We set the simulation pressure to 100 bar (10 MPa), corresponding to a ~7.5 km depth beneath Europa's surface.

*Equilibrium Crystallization Simulations.* These simulations pertain to slow freezing in a spherical well-mixed chamber. The ice was assumed to form along the chamber walls in a uniformly thick layer, whereas the crystallized salts were assumed to remain in the central briny pocket and could continue to participate in chemical reactions.

A constant chamber size was assumed once salts started to precipitate; actual volume variations were on the order of a few percent. Most simulations proceeded to temperatures where there remained only a few percent (< 12%) of the initial solution mass, corresponding to the central pocket having < 50% of the initial chamber radius.

The solids formed include amorphous silica; Ca-, Mg-, and Na-sulfates (respectively gypsum, meridianiite, and mirabilite) and -carbonates (respectively calcite and ikaite, dolomite and magnesite, and nahcolite); and sodium and potassium chloride. Initial carbonate-to-sulfate ratios are of order 1 across the three main end-member compositions of [8]. Sodium carbonate (nahcolite) seems to form only if sodium is initially much more abundant than calcium and magnesium. Otherwise, Na readily combines with sulfate to form mirabilite. Ca and Mg preferentially form carbonates. Ca-sulfate (gypsum) is scarce even if Ca dominates the solution composition along with Na, $SO_4$, and $CO_3$. Mg-sulfate (meridianiite) forms only in

carbonate-free simulations. For the other two, silica-rich, high-pH fluid endmembers of [8], there is comparatively little freezing and abundant amorphous silica forms at the exclusion of salts.

*Fractional Crystallization Simulations*. These simulations pertain to the cases of Fig. 1a and 1c, in which the formed salts can no longer equilibrate with the central brine. Generally, the simulations proceeded to similar final temperatures as equilibrium crystallization simulations, and the solids formed were qualitatively the same. An example simulation for a poorly mixed chamber (Fig. 1c) is shown in Fig. 2.

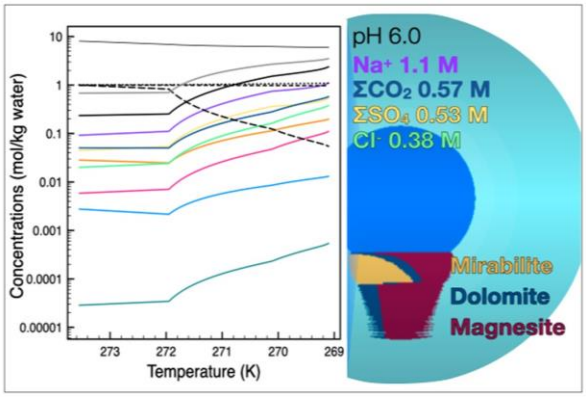


***Figure 2. Fluid compositions from end-member ocean compositions and modeling of their changes due to partial freezing in the shell.*** *Fluid composition (left) and spatial distribution of solution, ice, and salts in a freezing liquid reservoir at 100 bar (10 MPa) with a starting composition obtained from the `EM-CM' model of [8]. Here, salts are assumed to partition from ice and settle by density as in Fig. 1c. The compositions and spatial arrangement are independent of spatial scale.*

The non-ice solid precipitation sequence tends to be silica, followed by carbonates and/or sulfates, with chlorides forming last owing to their high solubility and ability to keep brine liquid at low temperatures.

Initial fast freezing, which would partially trap salt in ice [9], was ignored but can be inferred from redistribution of salts formed early in fractional simulations along the outer chamber wall (Fig. 1a).

**Discussion:** *Applications to Cylindrical Crack and Global-Scale Ocean Freezing.* The case of solid partitioning in an open fracture in an ice shell is a simplification of the spherical chamber case as the crack is still communicating with the ocean and only the onset-of-ice-formation temperature is considered. The case of a global ocean freezing is similar to that of a spherical chamber in terms of compositional evolution. If the ocean is well-mixed, the salts are distributed throughout the liquid much like the well-mixed chamber case, with the exception of the presence of a solid core surrounded by the ocean.

*Implications for Two-Way Transport in Ice Shell.* Salts tend to be denser, more insulating, and stronger than water ice. This can affect the propensity for fracturing and convection within an ice shell, affecting surface-to-ocean exchange. Viscosity appears to be the mechanical property that varies the most across solids relevant to ice shells and is likely to dominate the influence of composition on the propensity for convective transport.

*Ice Shell Characterization by Future Missions.* Our characterization of solid distributions in ice shells, coupled with future modeling of transport processes that account for compositional effects, can inform upcoming measurements by missions like JUICE and Europa Clipper. Beyond sensing by multi-flyby and orbiting spacecraft, constraints on heterogeneities in the subsurface structure can also inform subsurface exploration.

*Habitability of Brine Pockets*. Our simulations quantify the water activity, salinity, and pH of brine pockets in ice shells. Considering a 248 K minimum temperature for microbial survival on Earth [10], the combined stresses due to salinity and pH may not preclude microbial inhabitance of some of the partially frozen solutions.

**Acknowledgments:** We thank J. Toner for helping us make the PHREEQC freezing routine easier to use. This work was supported by NASA's Solar System Workings program (#80NSSC20K0139). The PHREEQC inputs and thermodynamic data, including the spreadsheet and C implementations of the model used to determine spatial distributions, are available at https://github.com/MarcNeveu/frezchem and https://github.com/MarcNeveu/IceShellXtal.

**References:** [1] Parkhurst D. L. and Appelo C. A. J. (2013) *USGS Tech. Rep.*, 6A43. [2] Toner J. D. and Catling D. C. (2017) *J. Chem. Eng. Data*, *62*, 995–1010. [3] Toner J. D. and Catling D. C. (2017) *J. Chem. Eng. Data*, *62*, 3151–3168. [4] Toner J.D. and Sletten R.S. (2013) *Geochim. Cosmochim. Acta.*, *110*, 84-105. [5] Marion G.M. (2001) *Geochim. Cosmochim. Acta.*, *65*, 1883-1896. [6] Marion, G.M. et al. (2005) *Geochim. Cosmochim. Acta.*, *69*, 259-274. [7] Marion, G.M. et al. (2011) *Icarus*, *212*, 629-642. [8] Melwani Daswani, M. et al. (2021) *Geophys. Res. Lett.*, *48*, e2021GL094143. [9] Buffo J. et al. (2020) *J. Geophys. Res. Planets*, *125*, e2020JE006394. [10] Merino N. et al. (2019) *Front. Microbiol.*, *10*, 780.